Mechanism and Machine Theory 44 (2009) 2053–2065

Contents lists available at ScienceDirect

Mechanism and Machine Theory

journal homepage: www.elsevier.com/locate/mechmt

Geometrical aspects of double enveloping worm gear drive

L.V. Mohan, M.S. Shunmugam *

Manufacturing Engineering Section, Department of Mechanical Engineering, Indian Institute of Technology Madras, Chennai 600 036, India

ARTICLE INFO

Article history:
Received 10 November 2008
Received in revised form 16 May 2009
Accepted 21 May 2009
Available online 13 June 2009

Keywords:
Double enveloping worm
Contact pattern
Fly-cutting tool

ABSTRACT

Double enveloping worm gearing is expected to have contact over larger number of teeth and higher load carrying capacity compared to single enveloping worm gearing. In this paper, contact in this gearing is analysed by geometrical simulation of worm gear tooth generation using intersection profiles of different axial sections of worm representing the hob tooth profile with transverse plane of worm gear. The analysis reveals that in the engaging zone a straight line contact always exists in the median plane and intermittent contact exists at the extreme end sections of worm. This has lead to the idea of using two fly cutters positioned at the location identical to the extreme end sections of worm to generate full worm gear tooth thereby eliminating the need for hobs of complex geometry. For a given worm, a mating worm gear is machined in a gear hobbing machine using fly tool in two settings and nature of contact with the worm is checked by a blue test.

1. Introduction

Worm gear drives are used to transmit motion and power between two mutually perpendicular non-intersecting axes with large reduction in a single step. Cylindrical worms with corresponding single enveloping worm gears are quite common in usage due to their simplicity in manufacturing and assembly. In heavy-duty applications, double enveloping (DE) worm gear drives are recommended owing to their large load carrying capacity compared to single enveloping worm gear drives [1]. In double enveloping worm gear drive, greater number of teeth is in contact at any instant compared to single enveloping cylindrical worm gear drive. This drive is also named after its inventor as Hindley Hour-glass worm gear drive. They are used in sugar mills and coal mines due to high resistance to tooth breakage and better lubrication conditions. However, they pose problems in manufacture and require precise assembly.

Cylindrical worm having straight sided profiles in axial section (referred to as ZA-type) is cut by a trapezoidal tool that is set in an axial plane and moved parallel to the axis, as in a thread-chasing operation on a lathe. Mating worm gear is machined by a hob having appropriate cutting elements lying on the cylindrical worm surface. When manufacture of a hob is not justified in view its cost, a fly tool can be used for cutting of cylindrical worm gear. However, a hobbing machine with a tangential feed is required to produce accurate worm gear. Also, it is a very slow process and can be used for machining worm gears, few in numbers. Without a tangential feed, fly cutter simply performs form cutting. For cutting a double enveloping worm, a trapezoidal tool set in axial plane is used with its edge always tangential to base circle while moving in a circular path concentric to gear axis. The mating double enveloping worm gear requires a hob resembling the double enveloping worm with cutting elements lying on the worm surface. Hobs with such complex geometry are difficult to manufacture.

It is presumed that due to the enveloping nature of worm, the contact in this gearing is over much larger area and greater number of teeth is in contact compared to single enveloping worm gear set. Earlier work reveals that in the engaging zone,

* Corresponding author. Tel.: +91 44 22574677; fax: +91 44 22570509.
E-mail address: shun@iitm.ac.in (M.S. Shunmugam).

0094-114X/$ - see front matter © 2009 Elsevier Ltd. All rights reserved.
doi:10.1016/j.mechmachtheory.2009.05.008

Nomenclature

b	half width of worm cutting tool at pitch circle
C	center distance
k	number of axial sections
m	module
n	gear ratio
r_b	base circle radius
r_p	pitch circle radius of worm gear at throat
$S_g(X_g, Y_g, Z_g)$	reference coordinate frame of worm gear
$S_w(X_w, Y_w, Z_w)$	reference coordinate frame of worm
$S_t(X_t, Y_t, Z_t)$	tool coordinate frame
$S_1(X_1, Y_1, Z_1)$	fixed coordinate frame on worm gear
$S_2(X_2, Y_2, Z_2)$	fixed coordinate frame on worm
t	distance of a plane from median plane
Z_w	number of start on worm
Z_g	number of teeth on worm gear
u	tool edge parameter
α	cutting edge/pressure angle
ϕ_1	tool rotation parameter
ϕ_2, θ_2, ψ_2	worm rotation parameters
θ_1, ψ_1	worm gear rotation parameter
ψ	angular disposition of axial plane

the contact is established as straight line in median plane of the worm gear irrespective of the rotation angle and intermittent contact appears on transverse end planes and central plane of the worm. Further it shows that the meshing action in this gearing is like cam action with more of sliding [2]. Review of literature shows that differential geometry approach is widely used to analyze this gearing [3–9]. However, it is also reported that an undercutting is performed by the extreme edge of the hob [10]. As differential geometry approach does not address the problem fully when interference or undercutting phenomenon exits in machining, intersection profile method as reported by Buckingham [2] is chosen. The nature of contact and undercutting phenomenon in generation of double enveloping worm gear is analysed by geometrical simulation of gear tooth profile generation using the different axial section profiles of the worm representing hob cutting edge geometry. A trace of intersection points of an axial section profile of worm with a transverse plane of worm gear on its generation is obtained with reference to fixed gear coordinate frame. This trace is called the intersection profile of particular axial section profile on a transverse plane under consideration as reported by Buckingham and Niemann in their books [2,11]. The inner envelope of such intersection profiles of different axial section profiles of worm obtained for a particular transverse plane of worm gear constitutes the worm gear tooth profile at the corresponding transverse plane. The analysis of generation of tooth profile at different transverse planes of worm gear shows that extreme end-sections of worm determine the worm gear surface. This has lead to the idea that fly cutters representing end tooth of hob are sufficient to machine the full worm gear tooth. In the present work, a single fly cutter is used to machine both the right and left flanks of the worm gear teeth in two settings. The contact pattern is also checked by a blue test with a mating worm in meshing.

2. Surface geometry

2.1. Worm surface

Fig. 1 shows the details of the double enveloping worm gear drive. Fig. 2 shows the coordinate frame used for analysis of double enveloping worm gear drive. Fig. 3 shows the coordinate systems used for obtaining worm surface. $S_t(X_t, Y_t, Z_t)$ and $S_w(X_w, Y_w, Z_w)$ are reference frames corresponding to tool and worm respectively. Coordinate frames $S_1(X_1, Y_1, Z_1)$ and $S_2(X_2, Y_2, Z_2)$ are rigidly connected to tool and worm respectively. A trapezoidal tool with basic rack profile, rotating about the gear axis produces the helicoidal surface on a kinematically linked worm blank rotating about its own axis. A right-hand single-start worm is considered in this study. Eq. (1) gives the right-side tool profile with parameter u and α. The reference (pitch) circle radius of the gear at throat is given by r_p and half-width of tool at the reference circle is given by b

$$p_1 = \begin{bmatrix} b + u\sin\alpha \\ -r_p + u\cos\alpha \\ 0 \\ 1 \end{bmatrix} \tag{1}$$

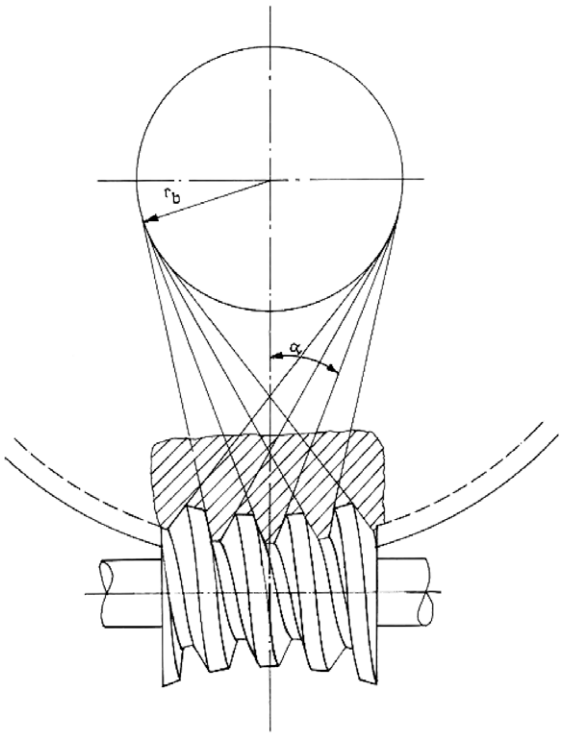

Fig. 1. Double enveloping worm gear drive.

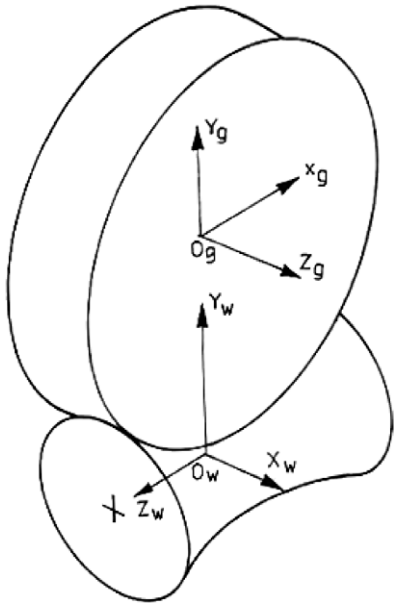

Fig. 2. Coordinate frame for double enveloping worm gear drive.

For left side tool profile, the values of α and b are taken as negative. The gear ratio n is defined as the ratio of number of teeth on the worm gear to number of start on the worm. This gives $\phi_2 = n\phi_1$, where ϕ_1 and ϕ_2 are rotation parameters of tool and worm respectively. The worm surface is obtained using coordinate transformation matrices as given by Eq. (2)

$$p_2 = [M_w^2][M_t^w][M_1^t]p_1 \tag{2}$$

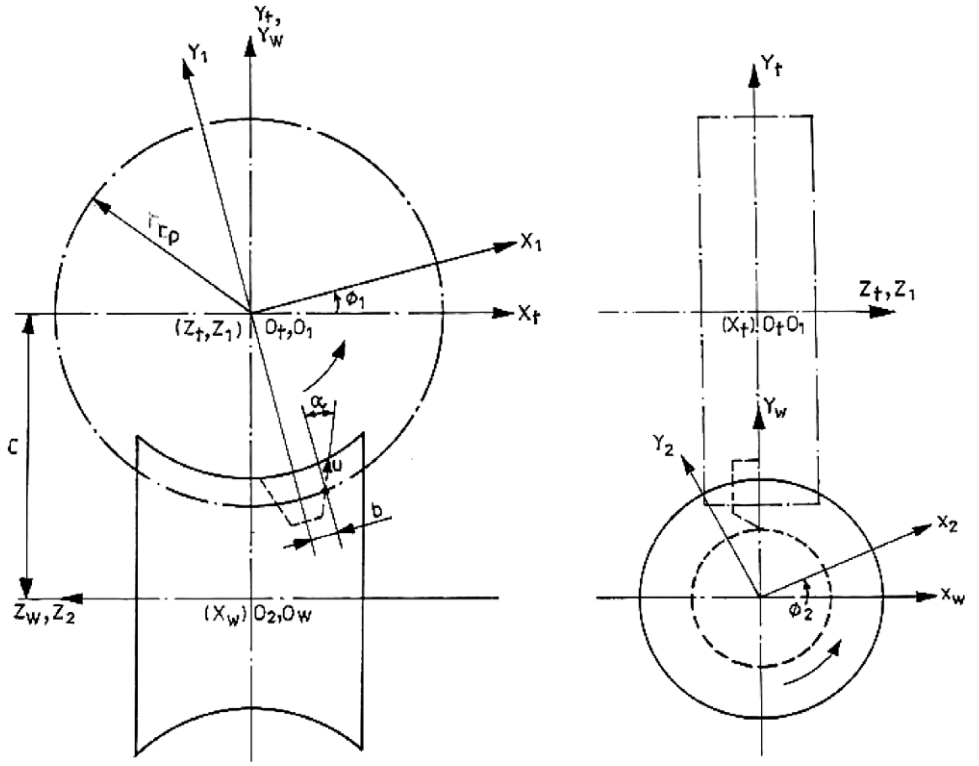

Fig. 3. Coordinate system to arrive at worm surface.

where

$$[M_1^t] = \begin{bmatrix} \cos\phi_1 & -\sin\phi_1 & 0 & 0 \\ \sin\phi_1 & \cos\phi_1 & 0 & 0 \\ 0 & 0 & 1 & 0 \\ 0 & 0 & 0 & 1 \end{bmatrix}; \quad [M_t^w] = \begin{bmatrix} 0 & 0 & 1 & 0 \\ 0 & 1 & 0 & C \\ -1 & 0 & 0 & 0 \\ 0 & 0 & 0 & 1 \end{bmatrix}; \quad [M_w^2] = \begin{bmatrix} \cos\phi_2 & \sin\phi_2 & 0 & 0 \\ -\sin\phi_2 & \cos\phi_2 & 0 & 0 \\ 0 & 0 & 1 & 0 \\ 0 & 0 & 0 & 1 \end{bmatrix}$$

Eq. (3) is the explicit form of representation of worm surface

$$p_2 = \begin{bmatrix} x_2 \\ y_2 \\ z_2 \end{bmatrix} = \begin{bmatrix} \sin\phi_2\{b\sin\phi_1 - r_p\cos\phi_1 + u\cos(\alpha-\phi_1) + C\} \\ \cos\phi_2\{b\sin\phi_1 - r_p\cos\phi_1 + u\cos(\alpha-\phi_1) + C\} \\ -b\cos\phi_1 - r_p\sin\phi_1 - u\sin(\alpha-\phi_1) \end{bmatrix} = \begin{bmatrix} A\sin\phi_2 \\ A\cos\phi_2 \\ B \end{bmatrix} \tag{3}$$

where $A = b\sin\phi_1 - r_p\cos\phi_1 + u\cos(\alpha-\phi_1) + C$ and $B = -b\cos\phi_1 - r_p\sin\phi_1 - u\sin(\alpha-\phi_1)$.

2.2. Worm gear surface

Worm gear surface is considered as a conjugate surface generated as an envelope of series of worm surfaces placed on the worm gear on its kinematic motion. From the principles of differential geometry, at any instant both envelope and the generating surface contact each other on a line and curve called characteristic or contact line [3]. Series of contact lines at different instances generate the worm gear surface. If a family of generating surfaces is represented by implicit form as $F(x, y, z, \theta)$ with θ as parameter of motion, then contact line can be determined by solving the Eq. (4) given below

$$F(x,y,z,\theta) = 0; \quad \frac{\partial F(x,y,z,\theta)}{\partial\theta} = 0 \tag{4}$$

Fig. 4 shows the coordinate systems used for generation of worm gear surface. Reference frames $S_g(X_g, Y_g, Z_g)$ and $S_w(X_w, Y_w, Z_w)$ correspond to worm gear and worm respectively. Coordinate frames $S_1(X_1, Y_1, Z_1)$ and $S_2(X_2, Y_2, Z_2)$ are rigidly connected to worm gear and worm respectively. Eq. (5) gives the surface coordinates of family of worm surfaces transformed to worm gear coordinate frame with kinematic parameters θ_1 and θ_2. As the gear ratio is n, θ_2 is represented in terms of θ_1 as $\theta_2 = n\theta_1$

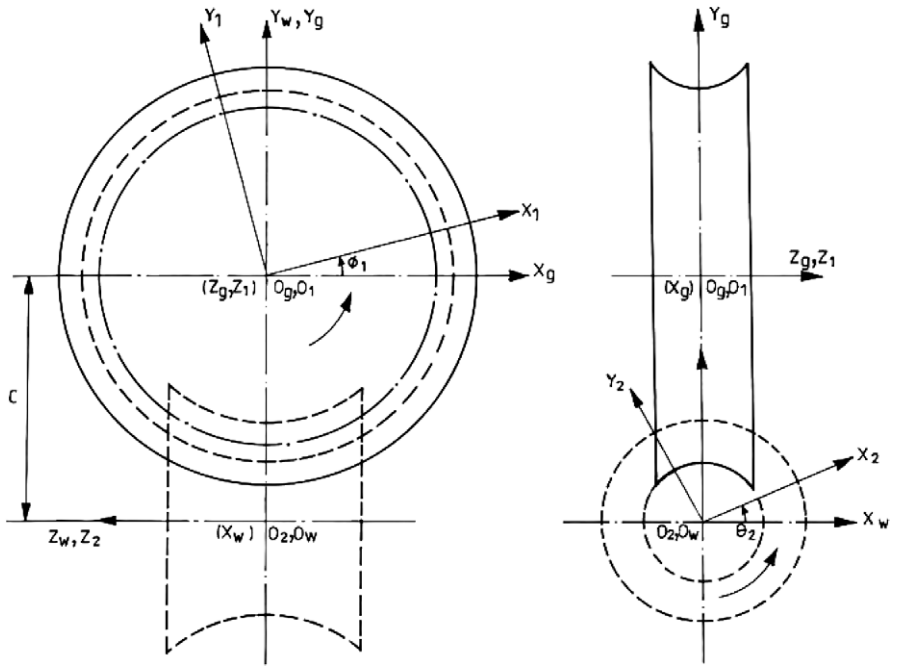

Fig. 4. Coordinate system to arrive at worm gear surface.

$$p_1 = [M_w^1][M_w^g][M_2^w]p_2 \tag{5}$$

where

$$[M_g^1] = \begin{bmatrix} \cos\theta_1 & \sin\theta_1 & 0 & 0 \\ -\sin\theta_1 & \cos\theta_1 & 0 & 0 \\ 0 & 0 & 1 & 0 \\ 0 & 0 & 0 & 1 \end{bmatrix}; \quad [M_w^g] = \begin{bmatrix} 0 & 0 & -1 & 0 \\ 0 & 1 & 0 & -C \\ 1 & 0 & 0 & 0 \\ 0 & 0 & 0 & 1 \end{bmatrix}; \quad [M_2^w] = \begin{bmatrix} \cos\theta_2 & -\sin\theta_2 & 0 & 0 \\ \sin\theta_2 & \cos\theta_2 & 0 & 0 \\ 0 & 0 & 1 & 0 \\ 0 & 0 & 0 & 1 \end{bmatrix}$$

The explicit form of the above equation is given as

$$\begin{bmatrix} x_1 \\ y_1 \\ z_1 \end{bmatrix} = \begin{bmatrix} A(\sin\phi_2 \sin\theta_1 \sin\theta_2 + \cos\phi_2 \cos\theta_2 \sin\theta_1) - B\cos\theta_1 - C\sin\theta_1 \\ A(\sin\phi_2 \sin\theta_2 \cos\theta_1 + \cos\phi_2 \cos\theta_1 \cos\theta_2) + B\sin\theta_1 - C\cos\theta_1 \\ A(\cos\theta_2 \sin\phi_2 - \sin\theta_2 \cos\phi_2) \end{bmatrix} \tag{6}$$

Eliminating A, B, ϕ_1 and ϕ_2 from Eq. (6), the implicit form of the equation is obtained

$$F(\theta_1) = \left\{ \left[(x_1 \sin\theta_1 + y_1 \cos\theta_1 + C)^2 + z_1^2 \right]^{\frac{1}{2}} - C \right\} \sin(\alpha - \phi_1) - (x_1 \cos\theta_1 - y_1 \sin\theta_1)\cos(\alpha - \phi_1) + b\cos\alpha + r_p \sin\alpha = 0 \tag{7}$$

where

$$\phi_1 = \theta_1 - \frac{1}{n}\cos^{-1}\left\{ \frac{(x_1 \sin\theta_1 + y_1 \cos\theta_1 + C)}{\left[(x_1 \sin\theta_1 + y_1 \cos\theta_1 + C)^2 + z_1^2 \right]^{\frac{1}{2}}} \right\} \tag{8}$$

Differentiating Eqs. (7) and (8) with respect to θ_1, we get Eqs. (9) and (10)

$$\begin{aligned} \frac{\partial F(\theta_1)}{\partial \theta_1} &= [(x_1 \sin\theta_1 + y_1 \cos\theta_1 + C)^2 + z_1^2]^{\frac{1}{2}} \cos(\alpha - \phi_1)\left\{ -\frac{d\phi_1}{d\theta_1} \right\} \\ &\quad + \frac{(x_1 \sin\theta_1 + y_1 \cos\theta_1 + C)(x_1 \cos\theta_1 - y_1 \sin\theta_1)}{[(x_1 \sin\theta_1 + y_1 \cos\theta_1 + C)^2 + z_1^2]^{\frac{1}{2}}} \sin(\alpha - \phi_1) + (x_1 \cos\theta_1 - y_1 \sin\theta_1)\sin(\alpha - \phi_1)\left\{ -\frac{d\phi_1}{d\theta_1} \right\} \\ &\quad + \cos(\alpha - \phi_1)(x_1 \sin\theta_1 + y_1 \cos\theta_1) = 0 \end{aligned} \tag{9}$$

$$\frac{d\phi_1}{d\theta_1} = 1 + \frac{1}{n}\frac{z_1(x_1\cos\theta_1 - y_1\sin\theta_1)}{(x_1\sin\theta_1 + y_1\cos\theta_1 + C)^2 + z_1^2} \tag{10}$$

To obtain the surface coordinates of the worm gear, Eqs. (7)–(10) have to be solved for different values of z_1 and rotation parameter θ_1.

The nature of contact at the median plane is obtained by substituting $z_1 = 0$ in Eqs. (7)–(10). Substituting $z_1 = 0$ in Eqs. (8) and (10), $\theta_1 = \phi_1$ and $\frac{d\phi_1}{d\theta_1} = 1$.

Substituting above values in Eq. (9), $(\alpha - \theta_1) = \frac{\pi}{2}$.

Substituting the above equality in Eq. (7), Eq. (11) is obtained. This represents an equation of a straight line corresponding to tool edge and is independent of the rotation parameter θ_1

$$\frac{x_1 - b}{y_1 + r_p} = \tan\alpha \tag{11}$$

This shows that there exits a straight line contact always on the median plane irrespective of the rotational position of the gear. Though it can be solved for median plane with $z_1 = 0$, for other planes these equations cannot be solved in a straightforward way. Hence, to understand the generation of gear tooth profiles at different transverse planes, geometrical simulation of gear tooth profile generation is carried out, using intersection profiles of different axial section profiles of worm groove at different angular positions. The procedure is explained briefly in next section.

3. Geometrical simulation of gear tooth generation

Different axial section profiles of worm groove representing the hob tooth profile and angularly disposed by angle ψ in a uniform manner are considered for the simulation. Intersection points of an axial section profile when crossing a transverse plane of worm gear on its kinematic motion are obtained with reference to the fixed gear coordinate frame. Plotting these points gives the intersection profile of the particular axial section profile of worm groove. Similarly the intersection profiles of different axial sections of worm groove are obtained and the inner envelope of all these intersection profiles gives the generated gear tooth profile.

The axial section profile coordinates of the worm surface are obtained for different values of rotation parameter using Eq. (3) by substituting the value of ψ for θ_2. Value of θ_1 is obtained from the relation $\theta_2 = n\theta_1$. If k axial sections are considered, then the value of ψ will be integer multiple of $360/k$ degree. The intersection profiles of these axial sections are obtained using homogenous coordinate transformation matrices. Considering an axial section at angle of ψ from the median plane of worm gear, the axial section is brought to the median plane by rotation of the worm through an angle ψ in the anti-clockwise direction. Fig. 5 shows that a point $p_2(x_2, y_2, z_2)$ on this axial section is moved to point $P(x, y, z)$ on the median plane by rotation of this axial section. The coordinate of point P on the right-flank of worm groove is obtained by

$$p = \begin{bmatrix} x \\ y \\ z \end{bmatrix} = \begin{bmatrix} \cos\psi & \sin\psi & 0 \\ -\sin\psi & \cos\psi & 0 \\ 0 & 0 & 1 \end{bmatrix} p_2 \tag{12}$$

When this point moves to point $P'(x', y', z')$ on a plane at a distance t from the median plane by rotation of worm through an angle θ_2, the worm gear also rotates through an angle θ_2/n anticlockwise for a right-hand worm. The coordinates of the rotated point in the worm reference frame S_w are given by

$$P' = \begin{bmatrix} x' \\ y' \\ z' \end{bmatrix} = \begin{bmatrix} -t \\ y\cos\theta_2 \\ z \end{bmatrix} \text{ where } \theta_2 = \sin^{-1}\left(\frac{t}{y}\right) \tag{13}$$

The point P' can be transferred to worm gear coordinate system as P'' by coordinate transformation matrices as given by Eq. (14) with values of $\theta_1 = \frac{1}{n}(\theta_2 + \psi)$

$$P'' = [M_g^1][M_w^g]P' \tag{14}$$

where

$$[M_w^g] = \begin{bmatrix} 0 & 0 & -1 & 0 \\ 0 & 1 & 0 & -C \\ 1 & 0 & 0 & 0 \\ 0 & 0 & 0 & 1 \end{bmatrix}; \quad [M_g^1] = \begin{bmatrix} \cos\theta_1 & \sin\theta_1 & 1 & 0 \\ -\sin\theta_1 & \cos\theta_1 & 0 & 0 \\ 0 & 0 & 1 & 0 \\ 0 & 0 & 0 & 1 \end{bmatrix}$$

In a similar way, transforming all the points for a particular axial section to the gear coordinate frame and plotting the transformed points, the intersection profile of the particular axial section is obtained. Intersection profiles of other axial sections of worm are also obtained following the above procedure. The inner envelope of all these intersection profiles represents the

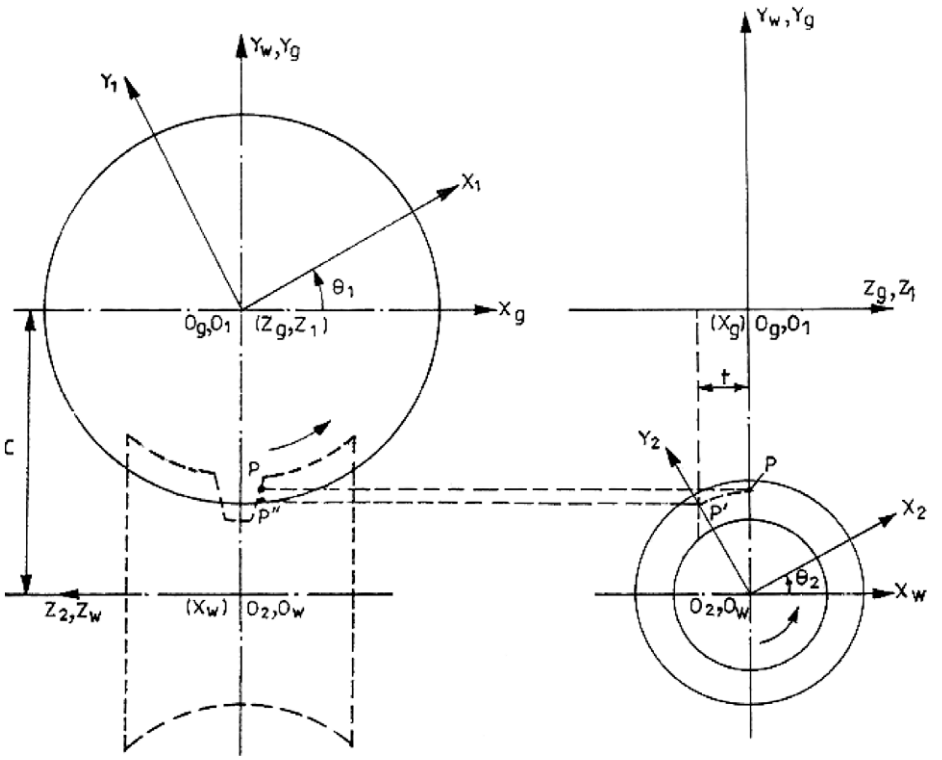

Fig. 5. Determination of intersection profiles.

gear tooth profile at that plane. Computer code is written in C for simulation of gear tooth profile generation and plot of the intersection profiles are made using MATLAB software.

3.1. Simulation case study

A case study of worm gear tooth generation using four axial sections of worm at 90° apart is considered in this study. The design details of worm and worm gear are given in Table 1. Two turns of the worm thread is considered with a total of nine axial section profiles as shown in Fig. 6. Initial position of axial section of worm groove with its flanks equally displaced on both sides of the central plane is numbered as A_0 and other teeth in the clockwise direction have positive subscript with increasing order as A_1, A_2, A_3 and A_4. Similarly for anti-clockwise direction the teeth are given negative subscript as A_{-1}, A_{-2}, A_{-3} and A_{-4}. Intersection profiles of these nine axial sections at different locations are obtained for median plane and shown in Fig. 7. Intersection profiles of planes away form the median plane by a distance of 10 mm on both sides of the median plane are shown in Fig. 8.

It is seen from Fig. 7 that the intersection profiles of different axial sections of worm at the median plane of gear are merging into one profile. This gives the inference that in the median plane straight line contact exists irrespective of the rotational

Table 1
Design details of double enveloping worm and worm gear.

Design parameter	Value
Module (m)	2.5 mm
No. of start of worm (Z_w)	1
No. of teeth on worm gear (Z_g)	40
Cutting edge angle (α)	20°
Half tool width at pitch circle	1.9635 mm
Outer diameter of worm at throat	47.5 mm
Reference diameter of worm at throat	42.5 mm
Root diameter of worm at throat	36.5 mm
Addendum	1 module
Dedendum	1.2 module
Centre distance	71.25 mm
Worm length	39.9 mm

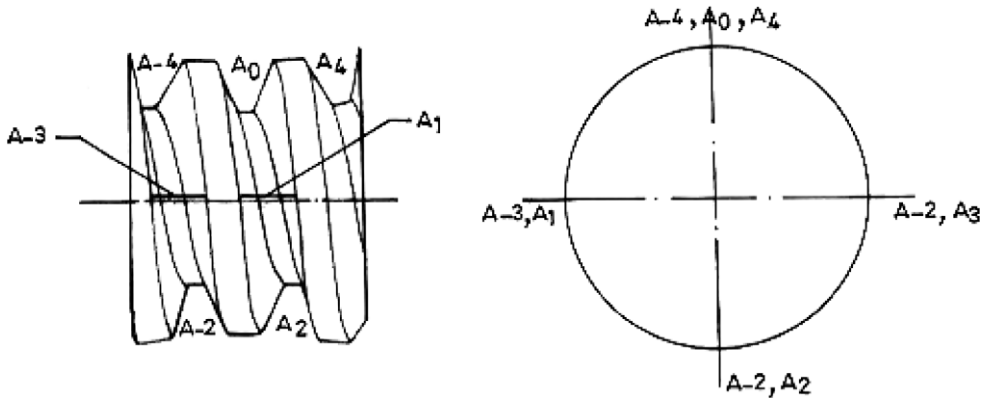

Fig. 6. Axial sections of worm.

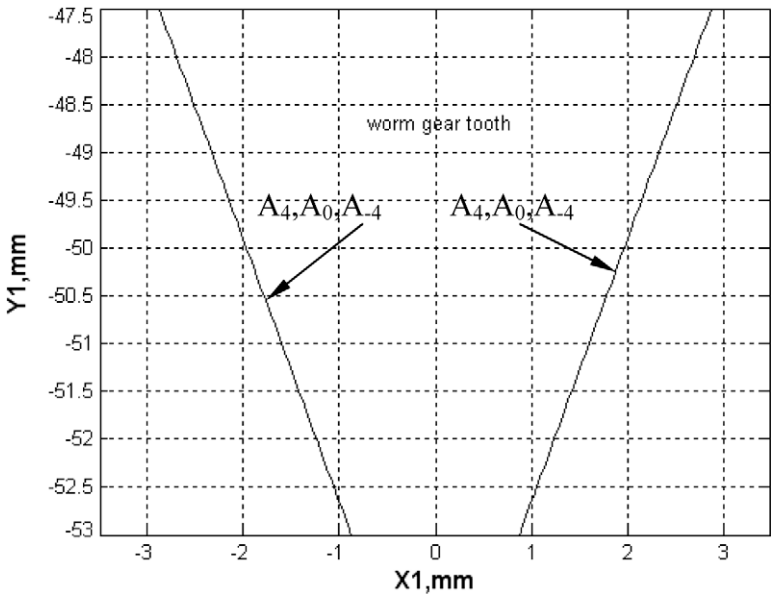

Fig. 7. Intersection profiles at median plane (double enveloping worm gear) (m = 2.5 mm, Z_g = 40, Z_w = 1, C = 71.25 mm, $\alpha = 20^\circ$).

position of the worm. In off-median planes, as seen from Fig. 8 the nature of intersection profiles and the resultant gear tooth profile reveals that there is no conjugate action. It is also seen from Fig. 8 that the resultant gear tooth profile is generated only by the intersection profiles of end axial sections A_{-4} and A_4. This shows that cutting is taking place by teeth represented by end axial sections A_{-4} and A_4. For planes oppositely displaced by equal distance from median plane, the gear tooth profile is found to be mirror image of the other. As these axial sections represent the hob teeth profile geometry with zero rake angle, it leads to an inference that one end-tooth of a hob is sufficient and both sides of the gear tooth can be obtained in two settings.

4. Contact between worm and gear

In order to study the contact for different rotational positions of worm, a worm gear generated by end axial-section (A_4) of worm is considered. The surface coordinates of the worm gear are obtained by substituting $\phi_2 = 2\pi$ in Eq. (6). Eq. (15) gives the surface coordinates of the right-flank of the worm gear tooth

$$\begin{bmatrix} x_{1r} \\ y_{1r} \\ z_{1r} \\ 1 \end{bmatrix} = \begin{bmatrix} A\sin\theta_1\cos\theta_2 - B\cos\theta_1 - C\sin\theta_1 \\ A\cos\theta_1\cos\theta_2 + B\sin\theta_1 - C\cos\theta_1 \\ -A\sin\theta_2 \\ 1 \end{bmatrix} \tag{15}$$

If the worm is rotated to an angle ψ_2, then the worm gear is rotated through an angle ψ_1 given by the relation $\psi_2 = n\psi_1$. The surface coordinates of right-flank of the worm groove at ψ_2 position for the axial section A_4 with $\phi_2 = 2\pi$ in gear reference coordinate frame S_g is given by Eq. (16)

$$\begin{bmatrix} x_{wr} \\ y_{wr} \\ z_{wr} \\ 1 \end{bmatrix} = \begin{bmatrix} 0 & 0 & -1 & 0 \\ 0 & 1 & 0 & -C \\ 1 & 0 & 0 & 0 \\ 0 & 0 & 0 & 1 \end{bmatrix} \begin{bmatrix} \cos\psi_2 & -\sin\psi_2 & 0 & 0 \\ \sin\psi_2 & \cos\psi_2 & 0 & 0 \\ 0 & 0 & 1 & 0 \\ 0 & 0 & 0 & 1 \end{bmatrix} \begin{bmatrix} 0 \\ A \\ B \\ 1 \end{bmatrix} = \begin{bmatrix} -B \\ A\cos\psi_2 - C \\ -A\sin\psi_2 \\ 1 \end{bmatrix} \tag{16}$$

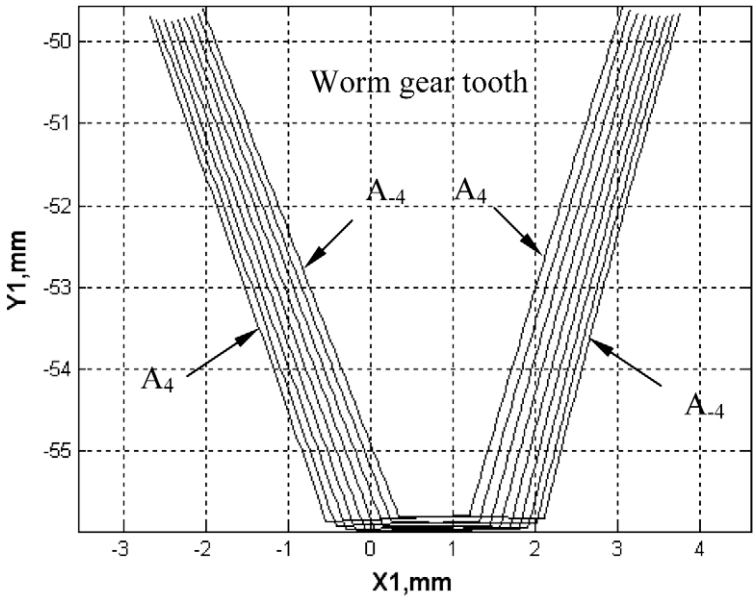

a) t = 10.0 mm (above median plane)

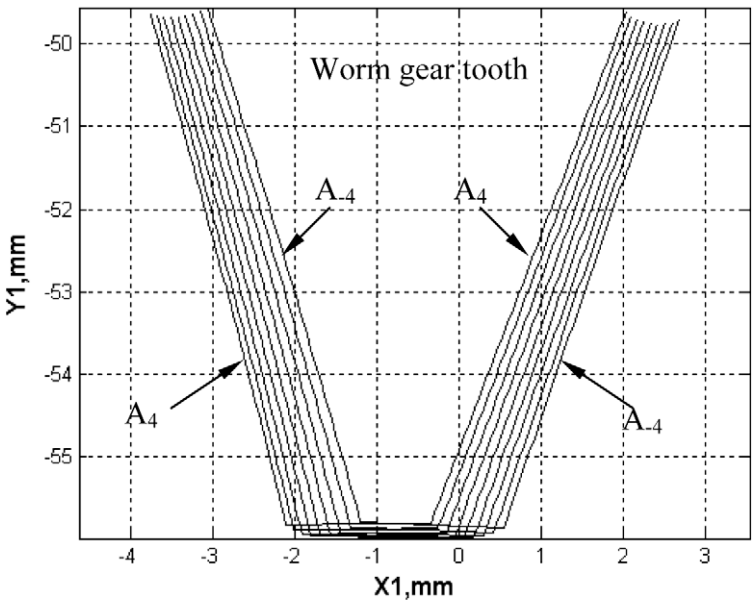

b) t = -10.0 mm (below median plane)

Fig. 8. Intersection profiles at off-median planes (double enveloping worm gear) (m = 2.5 mm, Z_g = 40, Z_w = 1, C = 71.25 mm, α = 20°).

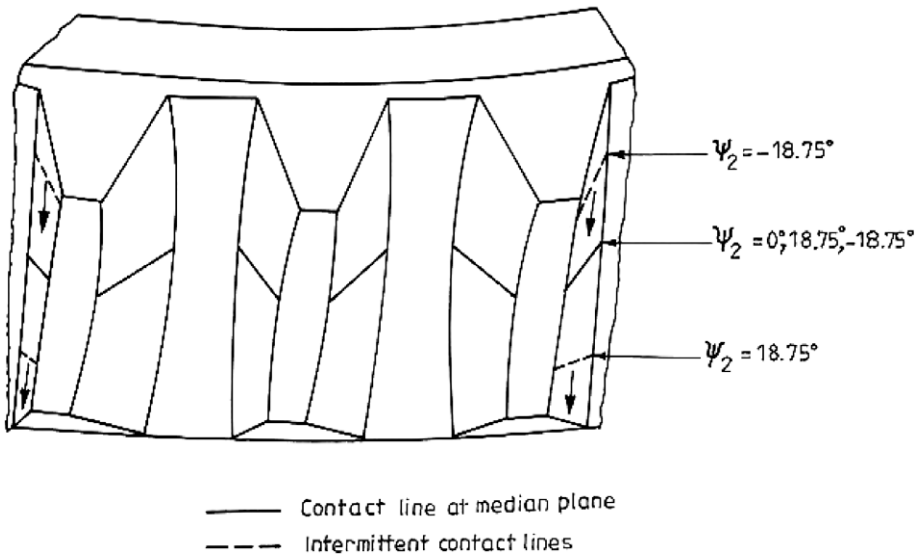

Fig. 9. Contact between double enveloping worm gear and worm.

The surface coordinates of the worm gear in the gear reference coordinate frame S_g for the rotated position ψ_1 is given by Eq. (16)

$$\begin{bmatrix} x_{gr} \\ y_{gr} \\ z_{gr} \\ 1 \end{bmatrix} = \begin{bmatrix} \cos\psi_1 & -\sin\psi_1 & 0 & 0 \\ \sin\psi_1 & \cos\psi_1 & 0 & 0 \\ 0 & 0 & 1 & 0 \\ & 0 & 0 & 1 \end{bmatrix} \begin{bmatrix} x_{1r} \\ y_{1r} \\ z_{1r} \\ 1 \end{bmatrix}$$

$$= \begin{bmatrix} \cos\psi_1(A\sin\theta_1\cos\theta_2 - B\cos\theta_1 - C\sin\theta_1) - \sin\psi_1(A\cos\theta_1\cos\theta_2 + B\sin\theta_1 - C\cos\theta_1) \\ \sin\psi_1(A\sin\theta_1\cos\theta_2 - B\cos\theta_1 - C\sin\theta_1) + \cos\psi_1(A\cos\theta_1\cos\theta_2 + B\sin\theta_1 - C\cos\theta_1) \\ -A\sin\theta_2 \\ 1 \end{bmatrix} \tag{17}$$

It is easily found that Eqs. (16) and (17) are same, if $\psi_2 = \theta_2$ and $\psi_1 = \theta_1$. The value of θ_2 assumes a value within the face width of the gear. This means that for any value ψ_2 within the range of θ_2, this contact exists as a sweeping intermittent contact on the right flank of the worm gear by the end axial section A_4 of worm. Besides this, contact always exists at the median plane irrespective of the rotation angle ψ_2. At $\psi_2 = 0$, the contact is only at the median plane in engaging teeth. With face width angle of 60°, for any other value of ψ_2 between −30° and 30° an intermittent contact lines starts from the top of the face width of the gear and sweeps the face width and disappears. As the left flank of axial section A_{-4} with $\phi_2 = -2\pi$ generates the left flank of the worm gear, similar intermittent contact exists on the left flank of worm gear tooth at this position. Fig. 9 shows the contact lines obtained in the median plane and intermittent contact with the end axial section A_4 of worm at $\psi_2 = 18.75°$ and $\psi_2 = -18.75°$ positions. For any values other than 2π or -2π of ϕ_2, the coordinates of Eqs. (16) and (17) do not coincide as the variables A and B have different values in these equations. This shows that there is no intermittent contact exists in other locations between the extreme end locations represented by 2π or -2π of ϕ_2. Thus for a face width angle of 60°, the intermittent contact exists in end sections for 60° only and for remaining 300° there does not exist any intermittent contact.

5. Machining of worm and worm gear

In order to verify the theoretical findings, the worm of double enveloping type is machined on a German make 'STAEHLY' gear hobbing machine with a trapezoidal form tool. Since the simulation studies carried out using a double enveloping worm with A_{-4}, A_{-3}, A_{-2}, A_{-1}, A_0, A_{+1}, A_{+2}, A_{+3}, A_{+4} sections (hob with nine cutting edges) show that the end sections A_{-4} and A_{+4} determine the final worm gear surface, the cutting edges placed at A_{-4} and A_{+4} positions must produce the worm gear surface. Therefore, a fly cutter with profile representing end tooth of the hob is used for worm gear machining.

Fig. 10a shows the tool holder assembled with form tool with included angle of 40° for machining worm in a gear hobbing machine. The worm blank is held in the hob spindle and the tool holder is mounted in the work spindle. Suitable change gears are selected to ensure the kinematic linkage between hob and work spindle based on the number of teeth in worm

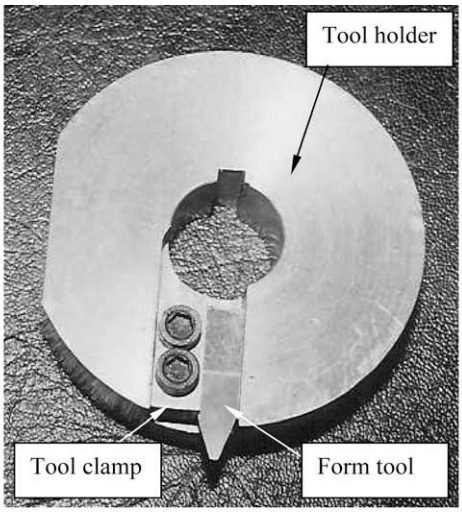

a) Tool assembly

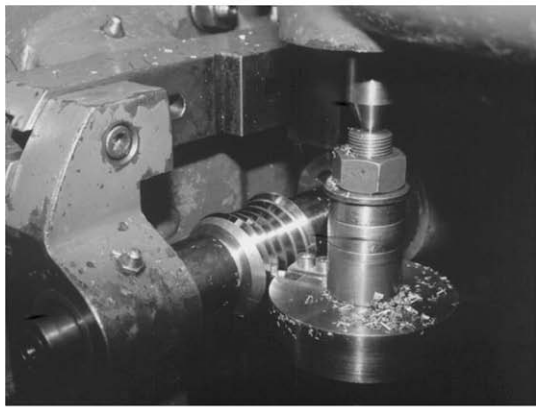

b) Machine set-up

Fig. 10. Machining worm of double enveloping worm gear set.

gear. Worm is progressively machined by radial feed only. Fig. 10b shows the machining set up for machining double enveloping worm in the hobbing machine.

The mating worm gear is machined with a fly tool of 49° included angle, which represents worm tooth angle. Fig 11a shows the fly tool assembled in the tool holder. In this case the tool holder in the hob spindle is set tangentially away from the gear axis so that at the median plane the tooth edge represents the end tooth of a hob. One flank of the worm gear is machined in this condition with radial feed to full depth. Then the worm gear is inverted and locked when the fly tool profile and machined worm gear tooth gap match at full depth in the median plane. The tool is retracted in the radial direction back to initial position and machining is carried out to cut the other flank of gear tooth. Fig. 11b shows the machining of mating worm gear in a gear hobbing machine with fly tool. It is also proved that a double enveloping worm gear can be machined with single fly tool thus eliminating the need for a geometrically complex gear hob.

5.1. Contact pattern by blue test

In order to obtain the contact pattern, the machined worm is mounted and locked with key and worm gear is mounted freely on the work spindle. The center distance is maintained and worm gear is centered and positioned with respect to the worm in the vertical and horizontal directions. Persian blue is applied on the worm gear teeth and worm is rotated in mesh with worm gear. Fig. 12 shows the contact obtained on the worn gear. It is inferred that the contact is established on the median plane as a straight line from gear tooth tip to root and this is in line with the results of the geometrical simulation study. Though intermittent contact exists in off-median plane theoretically and simulation studies also show its existence, it is not visible in the blue test. The reason may be that the worm gear is machined in two different settings and this setting error could have caused the contact pattern as observed in the blue test. It is also to be remembered that the contact pattern is also very sensitive to the mounting errors in the testing arrangement.

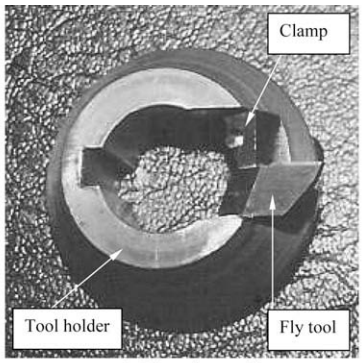

a) Fly tool assembly

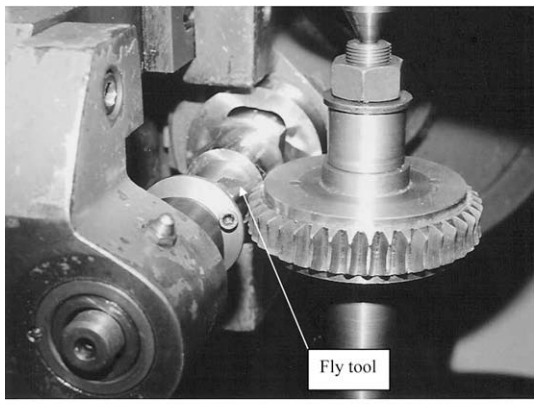

b) Machine set-up

Fig. 11. Machining worm gear of double enveloping worm gear set.

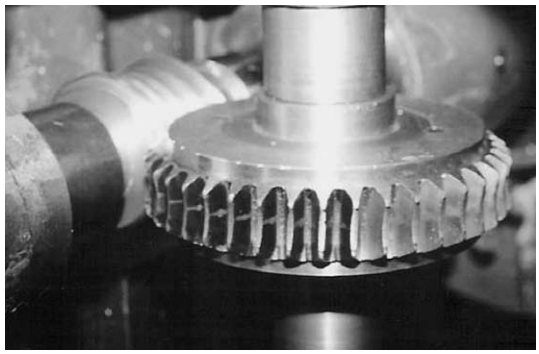

Fig. 12. Contact pattern by blue test.

6. Conclusion

Geometrical simulation of gear tooth generation carried out reveals that in this gearing the contact is established only on the median plane. The nature of intersection profiles of different axial sections of worm suggests that there is no conjugate action in off-median planes. It is also found from the simulation study that fly tools can be used to generate the worm gear. It is also shown by machining a mating worm gear of double enveloping worm that a single fly tool can be used to generate the worm gear thus eliminating the need for complex hobs. Theoretical findings show that intermittent contact exists at the extreme end sections of worms for a portion of angular rotation equal to face width angle of gear. This intermittent contact is not appearing in the assembly of machined sample pair due to the difficulty in matching the end plane of worm with the cutting edge location of fly tool in hobbing of worm gear.

References

[1] H.J. Watson, Modern Gear Production, Pergamon Press, New York, 1970.
[2] E. Buckingham, Analytical Mechanics of Gears, Dover Publications Inc., New York, 1949.
[3] M.L. Khanna, Differential Geometry, Jai prakash Nath & co., Meerut, India, 1990.
[4] S.G. Dhande, K.P. Karunakaran, Symbolic and computational conjugate geometry of a generic cutter and machine tool assembly, Journal of Design and Manufacturing 4 (1994) 167–186.
[5] F.L. Litvin, Theory of Gearing, 1212, NASA Reference Publication, 1989.
[6] W. Shi, D. Qin, W. Xu, Meshing control of the double-enveloping hourglass worm gearing under the conditions of existing the errors and the load, Mechanism and Machine Theory 39 (2004) 61–74.
[7] T. Sakai, M. Maki, H. Tamura, A study of hourglass worm gearing with constant slide-roll ratio, Transactions of the ASME 101 (1979) 274–280.
[8] V. Simon, Load distribution in double enveloping worm gears, Journal of Mechanical Design, Transactions of the ASME 115 (3) (1993) 496–501.
[9] V. Simon, Stress analysis in double enveloping worm gears by finite element method, Journal of Mechanical Design, Transactions of the ASME 115 (1) (1993) 179–185.
[10] F.L. Litvin, Alfonso Fuentes, Gear Geometry and Applied Theory, Cambridge University Press, United Kingdom, 2004.
[11] G. Niemann, Machine Elements, vol. II, Allied Publishers Pvt. Ltd., New Delhi, 1980.